

## Experimental investigation on process parameters of near-field deposition of electrospinning-based rapid prototyping

Deepak Parajuli, Pisut Koomsap, Alok A. Parkhi & Pitt Supaphol

**To cite this article:** Deepak Parajuli, Pisut Koomsap, Alok A. Parkhi & Pitt Supaphol (2016): Experimental investigation on process parameters of near-field deposition of electrospinning-based rapid prototyping, Virtual and Physical Prototyping, DOI: [10.1080/17452759.2016.1210314](https://doi.org/10.1080/17452759.2016.1210314)

**To link to this article:** <http://dx.doi.org/10.1080/17452759.2016.1210314>



Published online: 25 Jul 2016.



Submit your article to this journal



View related articles



View Crossmark data

# Experimental investigation on process parameters of near-field deposition of electrospinning-based rapid prototyping

Deepak Parajuli<sup>a</sup>, Pisut Koomsap<sup>a</sup>, Alok A. Parkhi<sup>a</sup> and Pitt Supaphol<sup>b</sup>

<sup>a</sup>Industrial and Manufacturing Engineering, School of Engineering and Technology, Asian Institute of Technology, Pathumthani, Thailand;

<sup>b</sup>Petroleum and Petrochemical College, Chulalongkorn University, Bangkok, Thailand

## ABSTRACT

Near-field electrospinning (NFES) with its capability to produce a straight fine fibre has been integrated into additive manufacturing for the fabrication of scaffolds with controllable pattern structures. However, building the third dimension with NFES is not easy due to the unsolidified fibre while being deposited. Presented in this paper is an investigation on the influence of process parameters on achieving a small cylindrical fibre from the near-field fibre deposition of an electrospinning-based rapid prototyping. A set of experiments have been conducted on solutions of polycaprolactone (PCL) in N,N-dimethylformamide (DMF). Parameters of interest are voltage, standoff distance, polymer concentration, environmental condition and needle size. From the experimental results, polymer concentration, environmental condition and needle size had influence on achieving a small cylindrical fibre. Under near-field deposition, the concentration should be high, the needle should be small and the temperature should be maintained during the process.

## ARTICLE HISTORY

Received 26 June 2016

Accepted 5 July 2016

## KEYWORDS

Scaffolds; tissue engineering; layer manufacturing technologies

## 1. Introduction

Near-field electrospinning (NFES) that stemmed from conventional far-field electrospinning (FFES) (Sun *et al.* 2006) has received much attention in recent years because it allows a deposition in a control fashion of a continuous fine fibre produced effortlessly from a stable polymer jet that is electrically drawn from a liquid polymer or polymer melt. The ability to control the pattern of the fibre deposition has been of researcher interest because it can help improve the performance of the conventional electrospinning that deposits the fibre randomly on a collector. For instance, in tissue engineering on which more than 40% of research publications on advanced applications of nanofibres are (Thavasi *et al.* 2008), electrospun fibres are used to construct scaffolds required to support cell attachment, proliferation and differentiation (Tellis *et al.* 2008). To perform their functions effectively, the fabricated scaffolds must meet not only mechanical and biological requirements but also structural requirements (Hasan *et al.* 2014). Porosity which is a space per a whole volume ratio should be high to contribute space for cells to attach and regenerate in all direction (Loh and Choong 2013) while a large pore size accommodates and delivers the cells for tissue regeneration (Too *et al.* 2002). Besides, pore interconnectivity is needed for the exchange of nutrients and gas,

and for the cells to penetrate into the scaffold structure. The random deposition of FFES, however, limits the ability to control the construction of internal channels within the scaffolds (Lam *et al.* 2002). As a result, the cells tend to grow on the surface instead of penetrating inside the scaffolds (Li *et al.* 2014).

Three-dimensional construction with controllable architecture by using electrospinning has been attractive for tissue engineering because electrospun fibres can mimic the fibre structure of natural extracellular matrix (Cai *et al.* 2013). Electrospinning has been applied with additive manufacturing for scaffold fabrication where electrospinning was used to create fine fibres while additive manufacturing techniques were used to control the architecture (Park *et al.* 2008, Chen *et al.* 2009, Owida *et al.* 2011). With direct writing capability of NFES, researchers have tried recently to fabricate 3D scaffolds directly from electrospinning. They are known under the names of electrohydrodynamic jet (EHD-jet) (Wei and Dong 2013), E-jetting (Li *et al.* 2014), electrospinning-based rapid prototyping (ESRP) (Chanthakulchan *et al.* 2015a) and electrohydrodynamic direct writing (EDW) (Zheng *et al.* 2016). These techniques are similar that they all follow fused deposition modelling process for a layer construction but instead of using extrusion process for fibre creation, NFES is applied to generate electrostatic force to draw a continuous fibre from a polymer solution or melt.

**Table 1.** Parameters classified based on influencing level on fibre diameter (Thompson *et al.*, 2007).

Major influence parameters	Moderate influence parameters	Minor influence parameters
Initial jet radius	Initial polymer concentration	Vapour diffusivity
Volumetric charge density	Perturbation frequency	Relative humidity
Standoff distance	Solvent vapour pressure	Surface tension
Initial elongational viscosity Relaxation time	Solution density	Electrical potential

The set-up of an equipment for NFES is similar to the conventional FFES, except that the standoff distance (SOD) is much shorter and the pattern is created by controlling the movement of the collector. When NFES was first introduced, the formation of a polymer droplet was done by dipping a wire tip in a solution (Kameoka *et al.* 2003, Sun *et al.* 2006). Later on a syringe needle has been applied for fast continuous deposition of a fibre for a large area (Chang *et al.* 2008, Bisht *et al.* 2011, Bu *et al.* 2012). The fibre stretching is created by the speed of the collector instead of the bending instability (Zheng *et al.* 2016). The faster the collector moves, the smaller the fibre diameter will be (Auyson *et al.* 2013). Chanthakulchan *et al.* (2015a) conducted experiments by using a solution of 10% weight of polycaprolactone (PCL) in N-dimethylformamide, and supplying 3.2 kV between a 20G needle with an inner diameter of 610 µm and a collector that were 5 mm apart. The experimental results showed the repeatability and reproducibility of the technique. However, deposited fibres remained in liquid state. The liquid fibres settled down to form a flat ribbon shape instead of a cylindrical shape. In case of multilayered fibre pattern, new layer was deposited on the previous liquid layer. Both the layers being in liquid state combined together to form one larger layer of scaffolds with lattice pores. Li *et al.* (2014) experienced similar results and reported much better control of the height of scaffolds at high PCL concentration in acetic acid (>70%w/v, PCL: acetic acid) when 2.2 kV was supplied between a 200 µm inner diameter nozzle and a collector that were 2 mm apart.

NFES benefits from the continuity of conventional electrospinning and superior location control to produce nanofibre patterns over larger areas. However, because the SOD is short, large amount of the solvent remains in the jet and majority of solidification process happens on the collector. Researchers have tried to solve this problem, for example, by increasing a flight time (i.e. to extend the straight part) by lowering voltage, and increasing viscoelasticity of the polymer solution (Bisht *et al.* 2011). Compared to the works on the conventional electrospinning, the process investigation has been much less. Presented in this paper is a study

**Table 2.** Average diameters of polymer jets and dry fibres at different supplied voltages.

Applied voltage level (kV)	Jet diameter (µm)	SD (µm)	Fibre diameter (µm)	SD (µm)	TR
3.2	57.15	0.69	162.54	2.80	2.84
3.5	53.08	1.20	168.14	2.80	3.17
3.7	55.24	1.31	159.74	5.60	2.89
3.8	57.55	0.69	162.54	5.60	2.82

**Table 3.** Average diameters of jets and dry fibres at different standoff distances.

Standoff distance (mm)	Jet diameter (µm)	SD (µm)	Fibre diameter (µm)	SD (µm)	TR
5	57.15	0.70	162.54	2.80	2.84
8	51.09	1.12	156.94	4.85	3.07
10	44.31	1.08	148.53	2.80	3.35
12	41.93	1.13	130.78	4.28	3.12
14	41.59	0.55	129.85	4.28	3.12

to have better understanding of near-field deposition in ESRP. A set of experiments were conducted to investigate the influence of process parameters on achieving small cylindrical fibres. The experiments were conducted in a particular sequence starting from voltage to SOD, polymer concentration, environmental condition and needle size. Next section reviews the parameters affecting the electrospinning process. Section 3 explains experimental set-up used for carrying out the experiments. Section 4 presents the experiments and results. The conclusions are addressed in the final section.

## 2. Literature review

The characteristics of electrospun fibres are influenced by several parameters that include solution properties (e.g. viscosity, conductivity, etc.), process parameters (e.g. electric potential, SOD, needle diameter, polymer concentration, etc.) and ambient conditions (e.g. temperature, humidity) (Doshi and Reneker 1995). For conventional electrospinning, significant change in fibre diameter occurs during bending instability when the fibre undergoes stretching and elongation (Rogina 2014). Intensive investigations have been conducted theoretically as well as experimentally on various types of materials. Thompson *et al.* (2007) for instance studied 13 parameters in an electrospinning theoretical model and determined their different effects on the fibre diameter as illustrated in Table 1. Majority of these parameters have an influence on enlarging the fibre diameter. Only SOD, elongational viscosity and solution density have an influence on reducing the diameter.

In case of NFES, there are few reports on the influence of parameters on the fibre diameter. Similar to the results from FFES (Katti *et al.* 2004, Gu *et al.* 2005), the influence

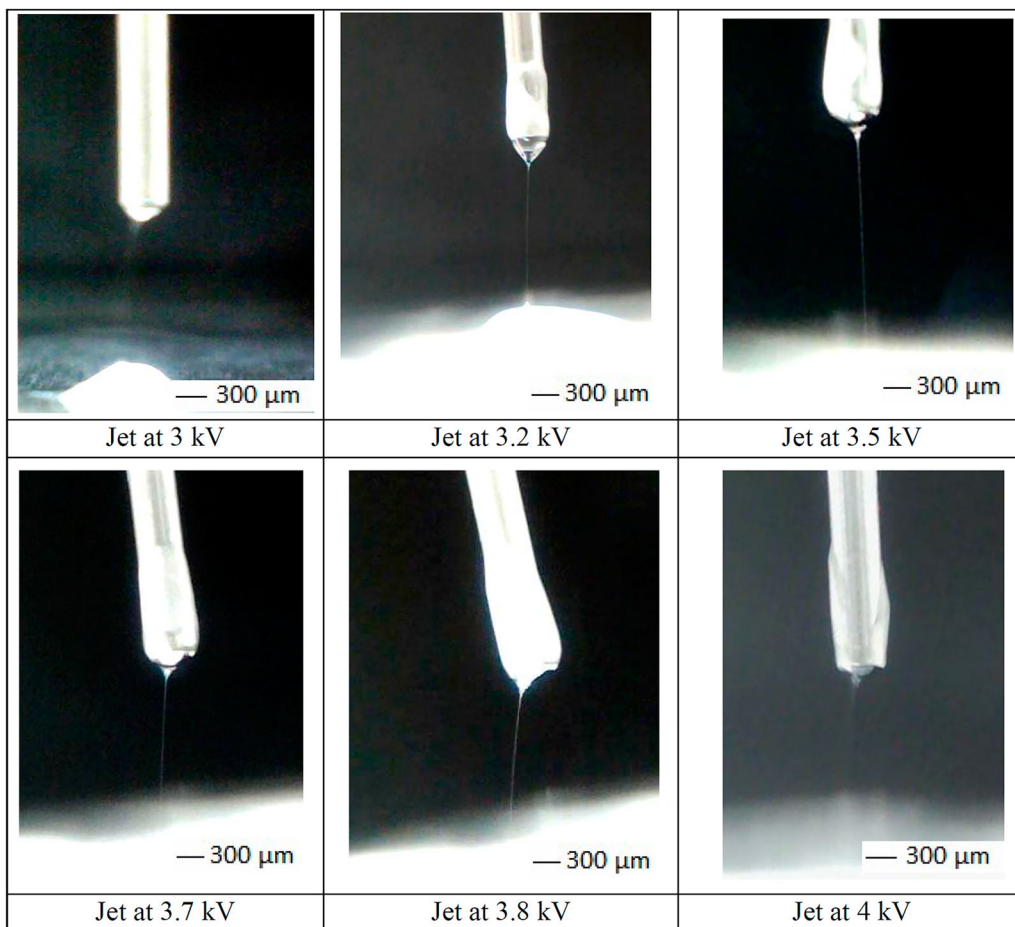


**Figure 1.** Polymer jet formation at different voltages.

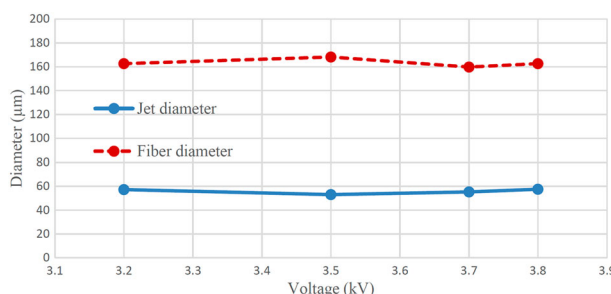


**Figure 2.** Comparison of jet's and dry fibre's diameters at different voltages.

of voltage is unclear also for NFES. One study reported slightly increase of the diameter when higher voltage was supplied (Bisht *et al.* 2011) while another reported insignificant effect on the diameter (Wei and Dong 2013). This might be because the real influencers to the diameter reduction are SOD and elongational viscosity, not the electric potential. Chanthakulchan *et al.* (2015b) reported that SOD has strong influence on the fibre diameter as it allows more time for the jet to be stretched although there is no instability bending. The

**Table 4.** Average diameters of jets and dry fibres at different polymer concentration levels.

Concentration level (%)	Jet diameter (μm)	SD (μm)	Fibre diameter (μm)	SD (μm)	TR
25	45.03	0.64	190.66	3.92	4.23
45	43.59	0.61	104.92	1.75	2.41
50	61.93	1.41	123.08	4.62	1.99
60	61.35	0.00	109.30	2.29	1.78
70	63.85	0.87	89.68	2.80	1.40
80	NA	NA	NA	NA	NA

longer the distance is, the thinner the fibre will be. They also reported that closed environment slightly affects the diameter while humidity has no influence. Padmanabhan *et al.* (2011) reported that polymer concentration has significant effect on increasing fibre diameters while needle size and electric field has insignificant effect. The combination of polymer concentration with electric field strength, however, has significant effect. Polymer concentration also helps improving control over the thickness of scaffolds (Li *et al.* 2014). Different results have been reported by Wei and Dong (2013) and Bain and Koomsap (2016) that needle size has

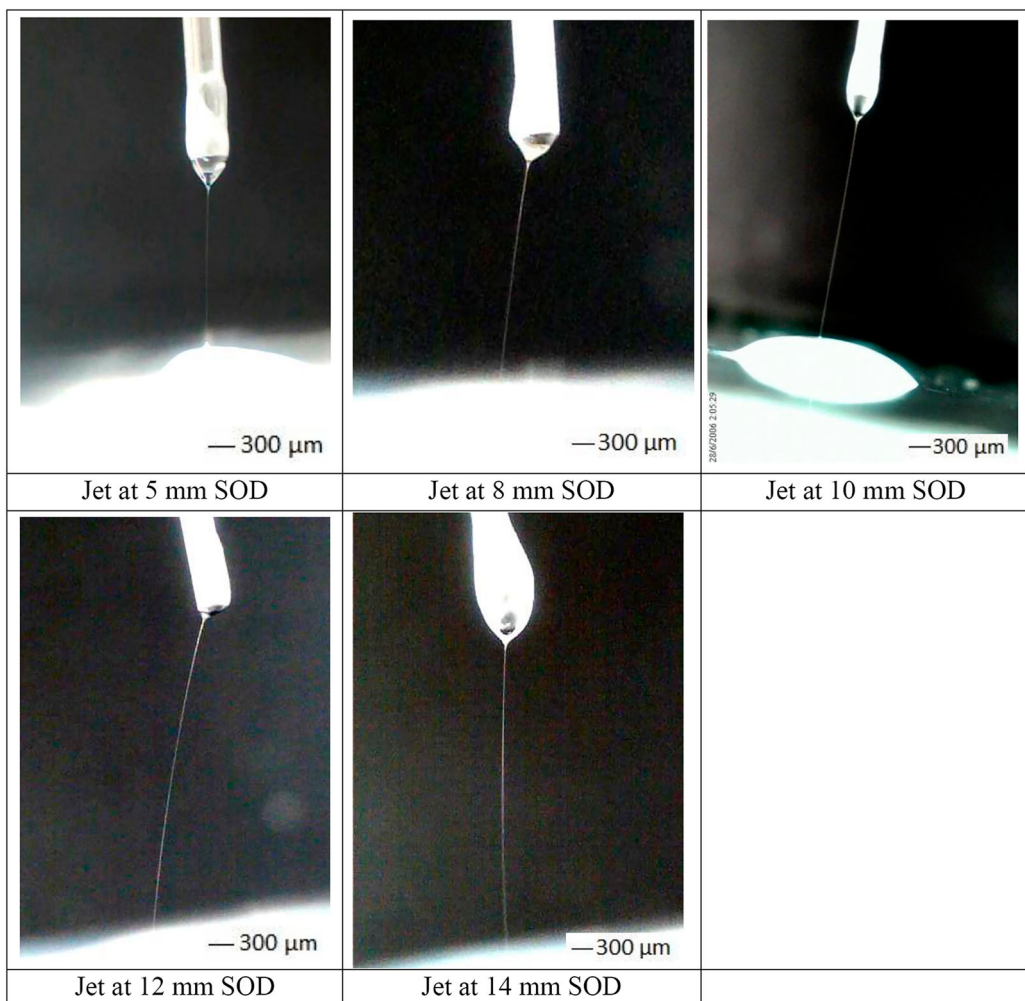


**Figure 3.** Polymer jet formation at different standoff distances.

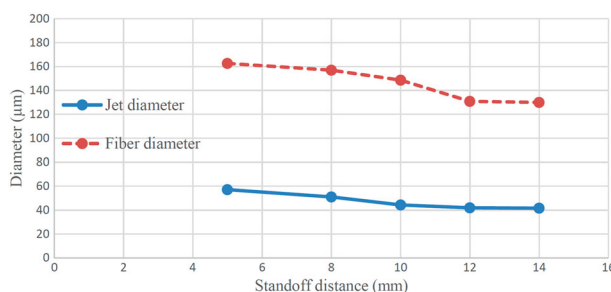


**Figure 4.** Comparison of jet and dry fibre diameters at different standoff distances.

strong influence on the fibre diameter as it directly relates to the initial size of the droplet. The speed of collector and material feed rate have also been reported to have direct influence on the size of the fibre (Bu *et al.* 2012, Wei *et al.* 2013, Zheng *et al.* 2016). Solvent has also been recently reported to have influence on the characteristic of the fibre as well as its diameter (Bain and Koomsap 2016).

### 3. Investigating influence of process parameters on ESRP

Since most of research activities on electrospinning have been on far-field deposition which also involves electrical bending instability period, the process conditions reported may not all be applicable to ESRP. Therefore, this study has been carried out to confirm some of the reported relationships, more importantly to gain understanding of the process conditions and to attempt to improve the process to attain a fine cylindrical fibre to support the fabrication of scaffolds with controllable patterns. As aforementioned, ESRP has adopted near-field deposition. This allows patterns to be created in a control fashion when a suitable pair of voltage and SOD is applied. The polymer jet has a cylindrical shape when it first comes out of the droplet (Koombhongse *et al.* 2001). To obtain the cylindrical shape, the fibre should solidify by the time it reaches the collector. Longer SOD will allow more time to the jet to dry. However, it is bounded to certain extent to control the straightness of

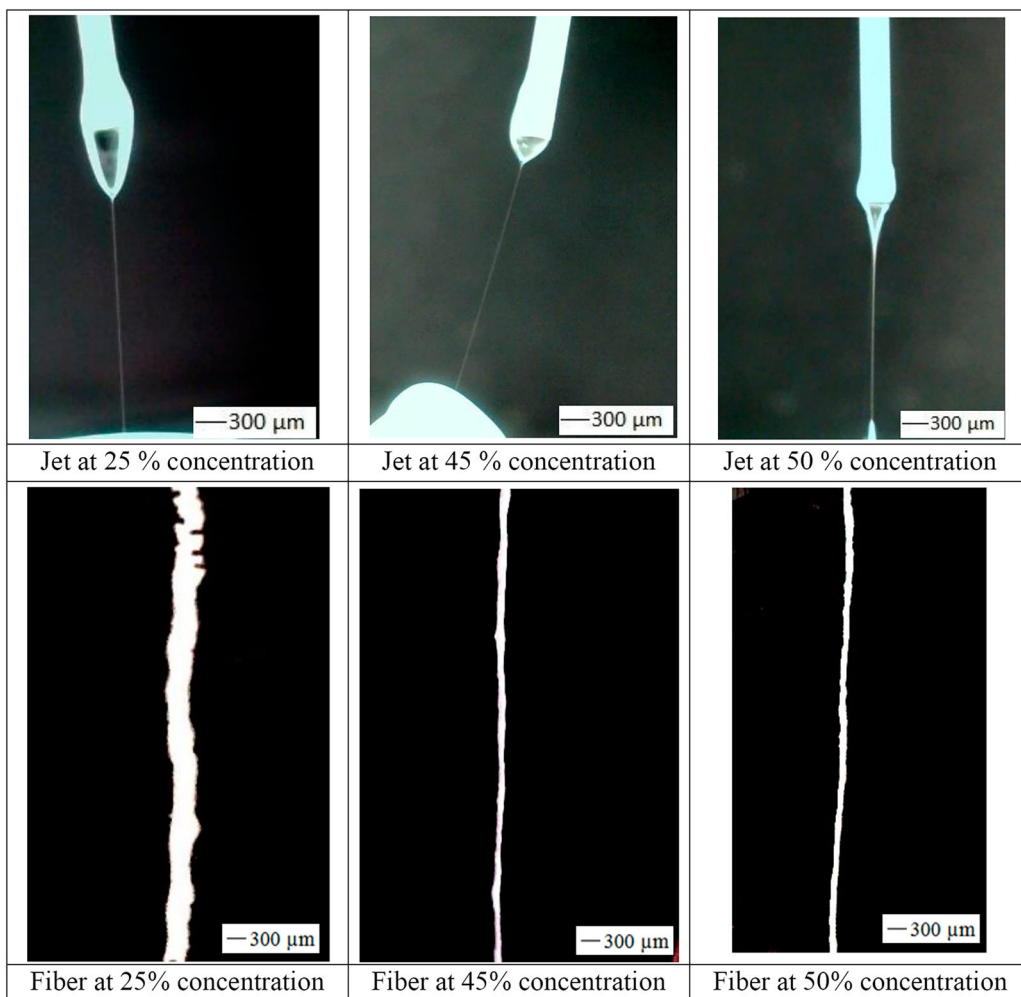


**Figure 5.** Polymer jets and dry fibres at 25%, 45% and 50% weight ratios of PCL in DMF.

**Table 5.** Average diameters of jets and dry fibres at different polymer concentration levels with warm air supplied.

Concentration level (%)	Jet diameter (μm)	SD (μm)	Fibre diameter (μm)			SD (μm)	TR
			NA	NA	NA		
25	NA	NA	NA	NA	NA	NA	NA
45	38.93	38.93	136.04	11.96	3.49	NA	NA
50	59.66	59.66	132.16	4.62	2.22	NA	NA
60	61.63	61.63	131.37	6.56	2.13	NA	NA
70	64.48	64.48	124.51	1.92	1.93	NA	NA
80	NA	NA	NA	NA	NA	NA	NA

the polymer jet. The solidification of the fibre also depends upon evaporation of solvent presence in the jet. The solvent should be evaporated quickly or the solvent should be kept at minimum in the solution, especially for short travelling. Environmental condition, especially temperature, can also have an influence on solvent evaporation. These parameters also contribute their influences on the fibre diameter.

Therefore, a set of experiments have been carried out to investigate the influences of electric potential, SOD, polymer concentration, fabrication condition and needle

**Table 6.** Average diameters of jets and dry fibres at different polymer concentration levels with compressed air supplied.

Concentration level (%)	Jet diameter (μm)	SD (μm)	Fibre diameter (μm)			SD (μm)	TR
			NA	NA	NA		
25	52.74	1.16	131.84	1.99	2.50	NA	NA
45	49.86	1.41	92.82	3.49	1.86	NA	NA
50	58.80	0.73	86.76	3.49	1.48	NA	NA
60	61.22	0.59	79.27	1.78	1.29	NA	NA
70	65.64	0.68	71.68	2.65	1.09	NA	NA
80	NA	NA	NA	NA	NA	NA	NA

size on polymer jets as well as their obtained fibres. A scaffold was fabricated with appropriate combination of these studied parameters. The experimental set-up is presented in the following subsections. The details of the experiments and results are available in the next section.

### 3.1. Experimental set-up

### 3.2. Material preparation

In this research, PCL with Mn 45,000 g/mol from Sigma Aldrich Chemistry was used as the polymer material for

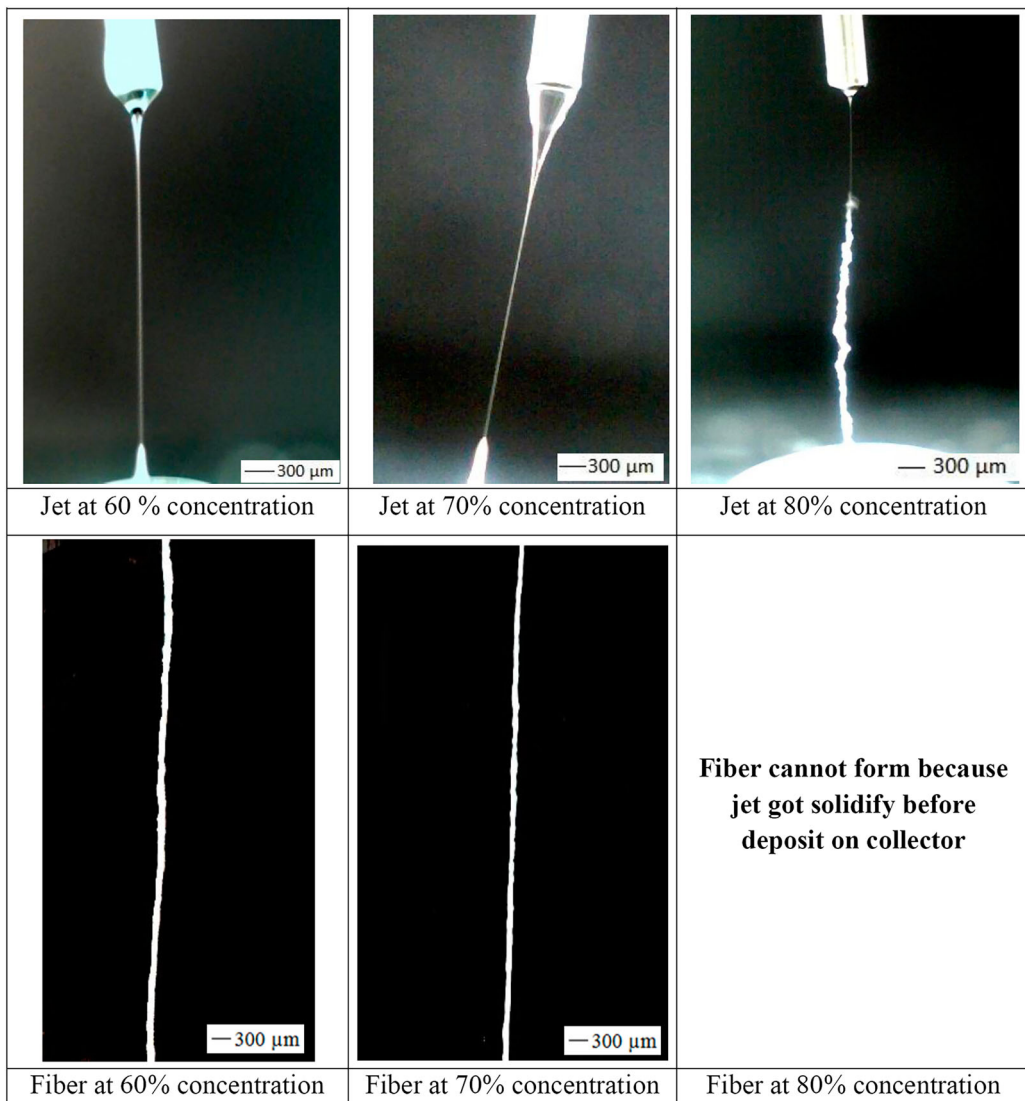


**Figure 6.** Polymer jets and dry fibres at 60%, 70% and 80% weight ratios of PCL in DMF.

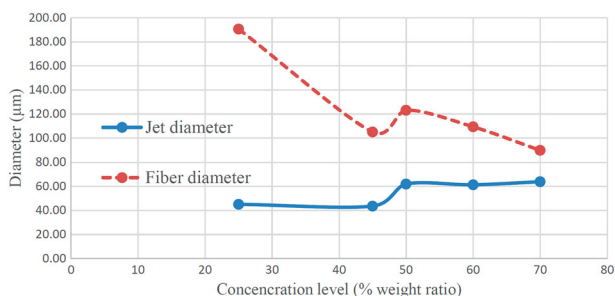


**Figure 7.** Comparison of jet and dry fibre diameters at different concentration levels.

the process. N,N-dimethylformamide (DMF) was used as a solvent. The polymer concentrations used in this study were from 10% to 80% weight ratio of PCL in DMF. For each concentration level, PCL and DMF were weighted on a digital scale. Both substances were mixed together

on a hot-plate stirring machine at the temperature of 80° C about 15 min. Each experiment was conducted after the solution's temperature was sat at room temperature for 30 min.

### 3.3. Machine set-up

An aluminium foil was placed on a collector platform. The positive charge line of a power supply was connected to the needle tip while the ground line was connected to the collector. For capturing the images of polymer jets, the collector was stationary. For creating fibres, the speed of the collector was fixed at 200 mm/s with acceleration and deceleration of 50 mm/s<sup>2</sup>. Three needle sizes were used in this study: 20G, 22G and 24G. The polymer solution was fed into the needle by gravity flow for the polymer concentration less than 50% weight ratio of PCL. Syringe pump was used for

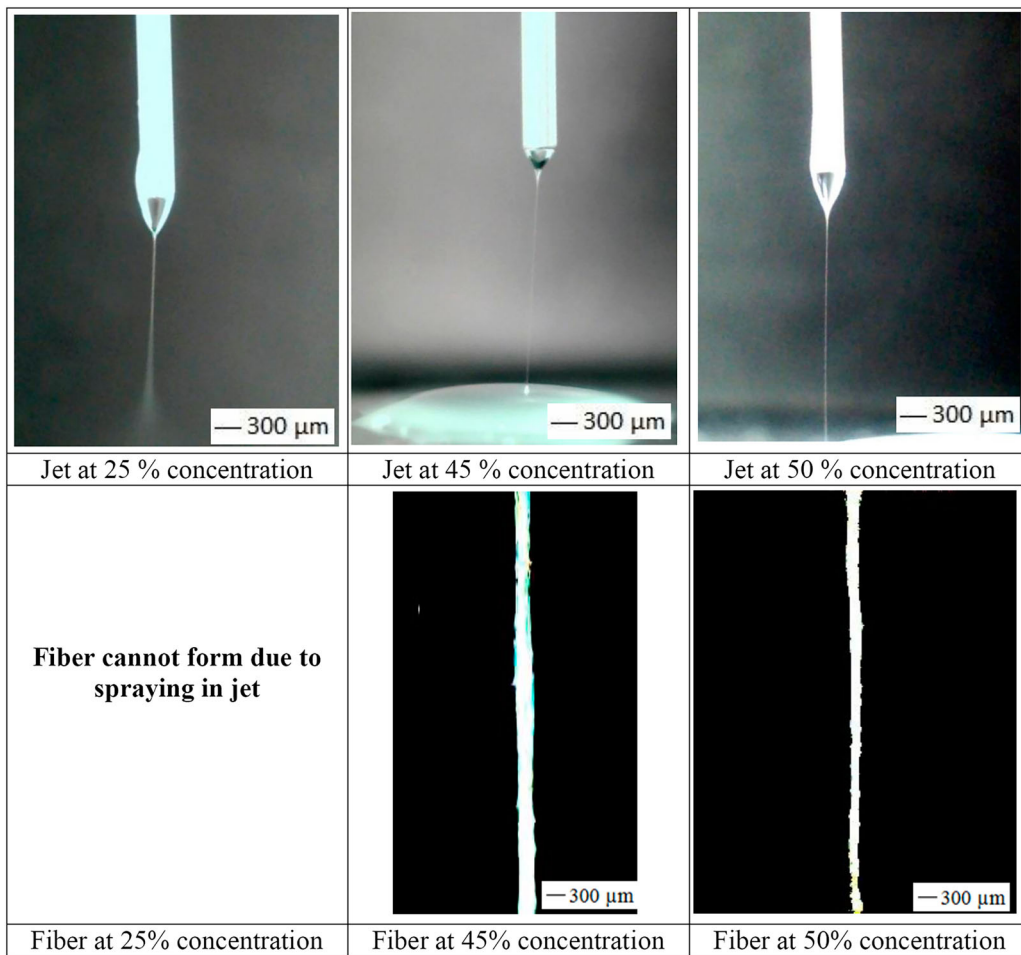


**Figure 8.** Polymer jets and dry fibres at 25%, 45% and 50% concentration levels with warm air supplied.

**Table 7.** Average diameters of jets and dry fibres created using 24G needle at different polymer concentration levels with compressed air supplied.

Concentration level (%)	Jet diameter ( $\mu\text{m}$ )	SD ( $\mu\text{m}$ )	Fibre diameter ( $\mu\text{m}$ )	SD ( $\mu\text{m}$ )	TR
25	36.07	0.66	110.80	2.70	3.07
45	41.35	0.86	71.22	2.97	1.72
50	50.12	1.14	69.25	2.56	1.38
60	53.00	1.66	65.89	1.78	1.24
70	55.48	2.18	59.96	2.86	1.08

feeding solutions with 50% weight ratio of PCL or higher because the solutions required assistance from an external force to flow through the needle. All experiments were conducted in closed environment.

### 3.4. Evaluation method

A portable digital microscope with MicroCapture software was used to capture the images of the polymer jets, dry fibres and fabricated scaffold. The diameters of the jets and dry fibres were determined relative to the known diameter of the needle taken under the same

conditions. Each experiment was repeated three times. Except for the first experiment on voltage, the measurements of the jets were taken at four different positions below the Taylor cone and the measurements of the dry fibres were taken at six different positions. The cylindrical shape of the obtained dry fibre was indirectly measured from the ratio of the dry fibre to the jet. In case that the fibre jet reaches the collector in a solid form, the diameter of the dry fibre on the collector should be about or smaller than the diameter of the jet. If the jet still contains liquid part, the diameter of the dry fibre on the collector will be larger than the jet. This is because the liquid part flows to the side. The cylindrical shape is then transformed to a ribbon shape.

## 4. Results and discussion

### 4.1. Voltage

Voltage is one of the factors which govern the continuous fibre formation process. Higher voltage is required

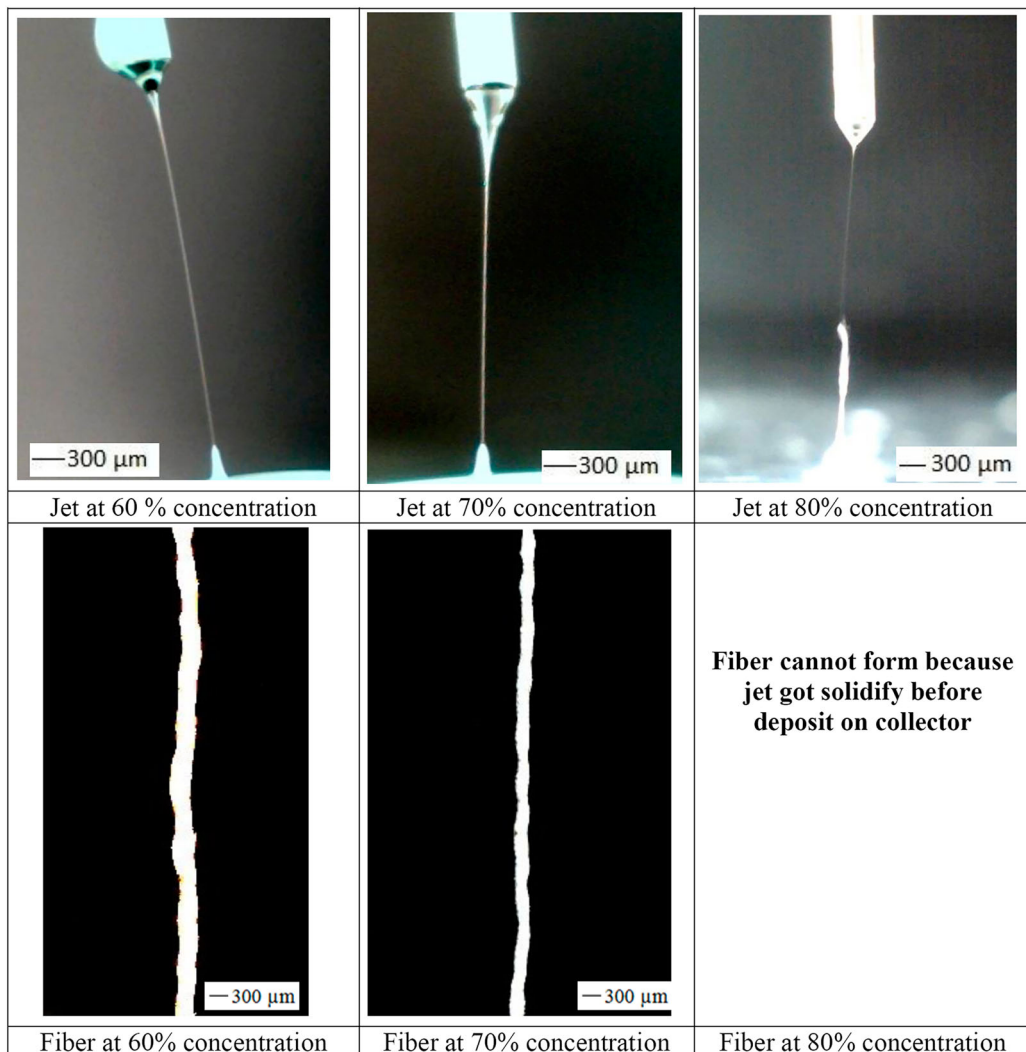


**Figure 9.** Polymer jets and dry fibres at 65%, 70% and 80% concentration levels with warm air supplied.

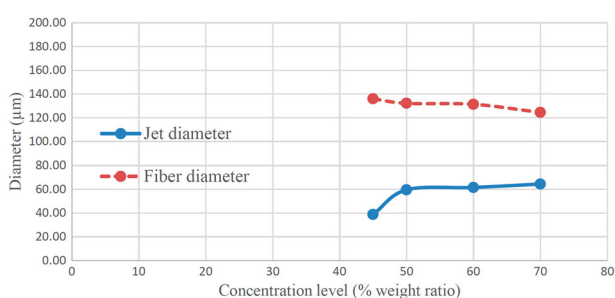


**Figure 10.** Comparison of jet and dry fibre diameters at different concentration levels with warm air supplied.

when SOD is increased, and a suitable range of voltages exists at every SOD for generating the polymer jet (Auyson *et al.* 2013). Applying voltage below the lower bound cannot form a jet and applying voltage beyond the upper bound will initiate uncontrollable multiple jets instead before disappeared. The first

experiment was conducted to study the influence of the voltage on the size of the polymer jet and of the dry fibre. The 20G needle was used and its tip was set 5 mm above the collector. Polymer concentration was 35% weight ratio. The study range was between 3 and 4 kV with the step increase of 0.2 kV. Relative humidity was around 65–70%. The results as illustrated in Figure 1 show that the proper range for creating fibres for this set-up was between 3.2 and 3.8 kV. Their images were captured. On the images, the diameters of the jets were measured at 2 mm below the tip of the needle. The average diameters are presented in Table 2 and Figure 2 which also present the average diameters of dry fibres created at these voltages. The results show that the variation of voltage did not cause a significant change in both jet's and dry fibre's size. It seems that the role of voltage was to initiate the polymer jet formation but it did not influence the jet diameter.

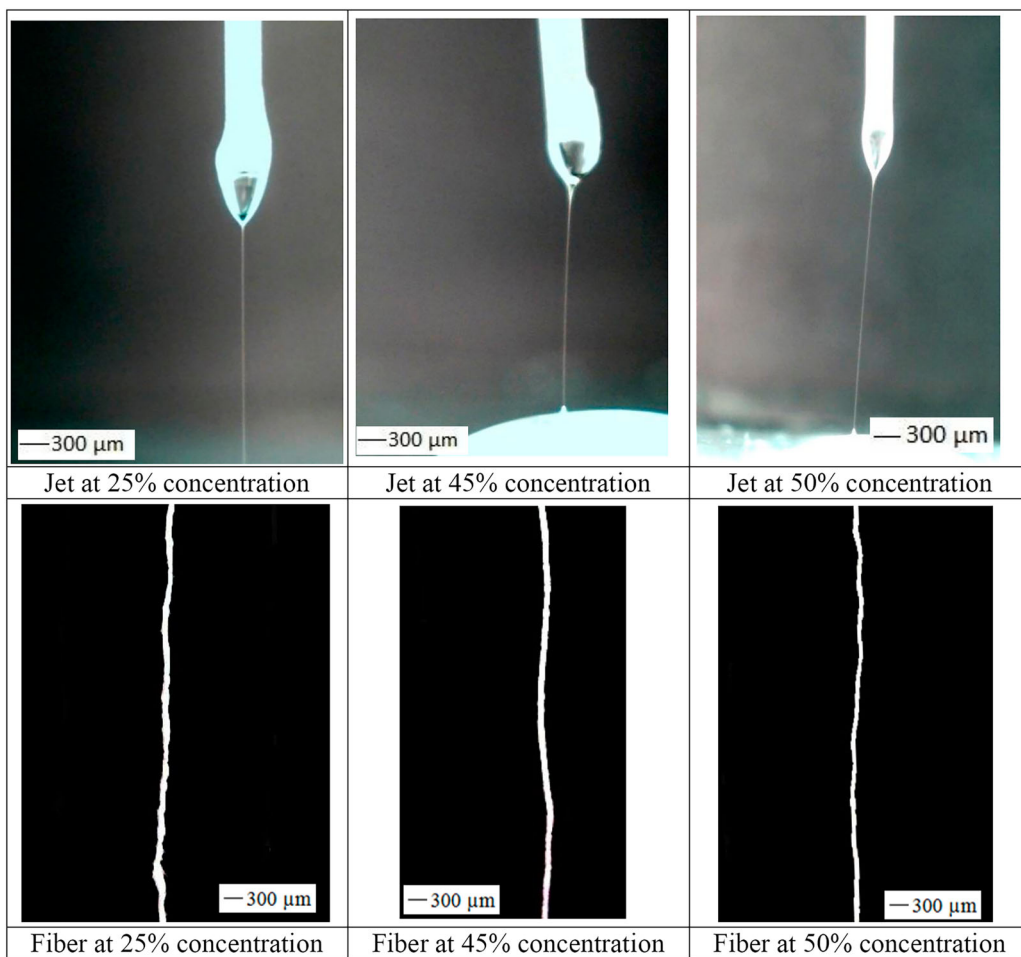


**Figure 11.** Polymer jets and dry fibres at 25%, 45% and 50% concentration levels with compressed air supplied.

#### 4.2. Standoff distance

As aforementioned, the recent study by Chanthakulchan *et al.* (2015b) on near-field deposition confirmed the influence of SOD on the fibre diameter. It stimulated a question whether the influence begins during the jet formation or after being deposited on the collector. This experiment was conducted to observe the influence of SOD on the size of the polymer jet. The experiment was similar to the previous one except the SOD was varied at four different SODs: 5, 10, 12 and 14 mm. The voltage was adjusted accordingly. Relative humidity was around 65–70%. The measurement on the jets was done underneath the Taylor cone when the diameters become more uniform. Fibres were also fabricated under these conditions. The results are presented in Figure 3 and Table 3. It can be seen that the diameters of both the jets and dry fibres decreased when the SOD increased. However, the gap between their diameters as shown in Figure 4 was large and pretty much unchanged. It means that the distances were too short for all

solvents to evaporate. Therefore, reduction of the solvent should be considered. It was also observed during the experiment that running the process at distance beyond 10 mm was not steady. The straight jet could not be achieved occasionally.

#### 4.3. Polymer concentration

This section presents a study on the influence of concentration on jet's and dry fibre's diameter and on the shape of the fibre. For this particular experiment, the 20G needle was used, and the SOD was 10 mm. Relative humidity was around 65–70%. Our preliminary study indicated that the minimum polymer concentration for creating a fibre was 25% weight ratio of PCL in DMF. The solution with lower concentration could flow through the needle but could not create a fibre. The maximum concentration was 45%. The solution with higher concentration could not flow through the needle with gravity flow. As a result, the syringe pump was used for continuing study on the influence of the

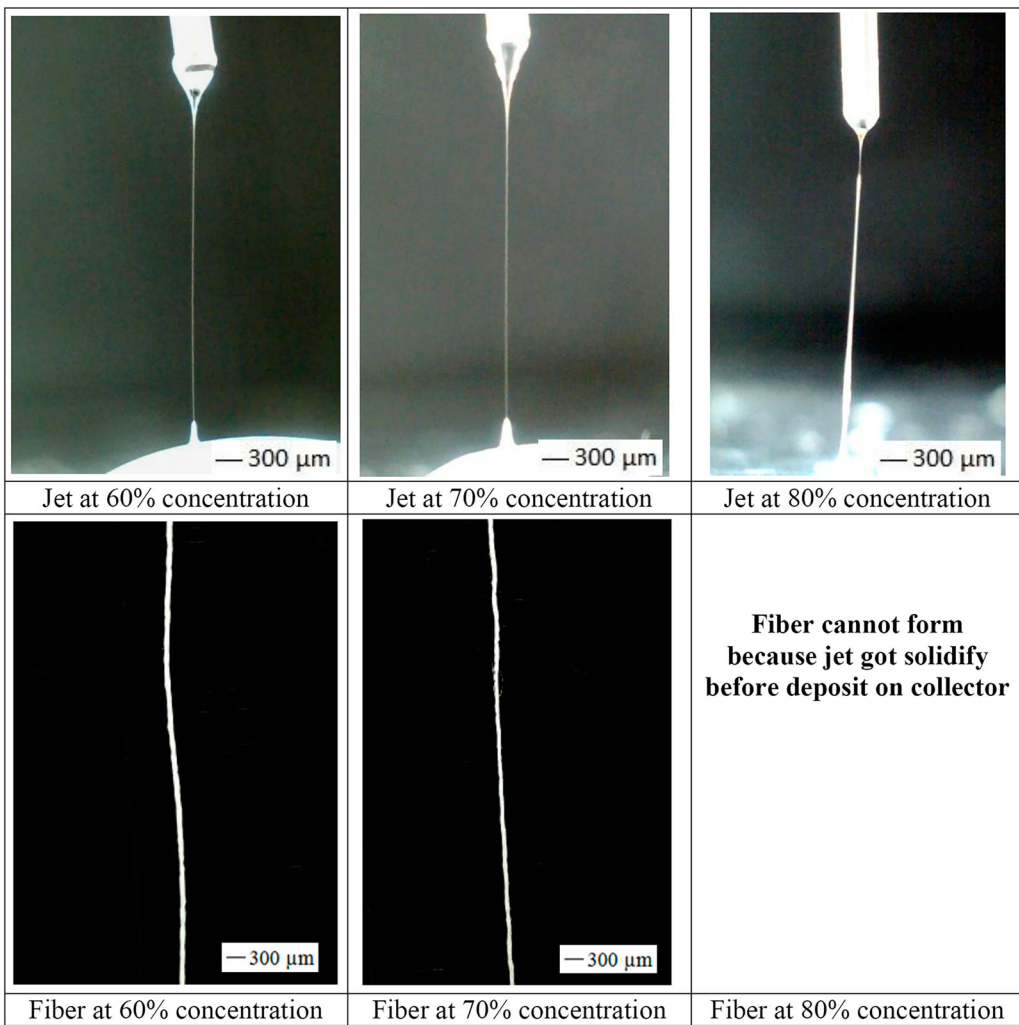


**Figure 12.** Polymer jets and dry fibres at 65%, 70% and 80% concentration levels with compressed air supplied.

concentration of 50% and higher. A feed rate was 1.21  $\mu\text{l/s}$ . The supplied voltage was between 3.2 and 3.5 kV for the concentration up to 50% weight ratio of PCL, and between 3.8 and 4.0 kV for higher concentration.

Figures 5 and 6 show the images of the jets and the dry fibres obtained at various concentration levels. The jet could be formed successfully but the fibres could be achieved up to 70% weight ratio of PCL in DMF. For the solution of 80% weight ratio of PCL, the jet solidified quickly prior to reaching a collector and prohibited the formation of a fibre on the collector.

Table 4 presents the measurement results. It is clear that both the jet and dry fibre diameters increased when the external force was provided as illustrated in Figure 7. However, the influence of concentration seemed to be insignificant on the jet but it had significant influence on the dry fibre diameter. The fibre diameter at 70% weight ratio of PCL was smaller than

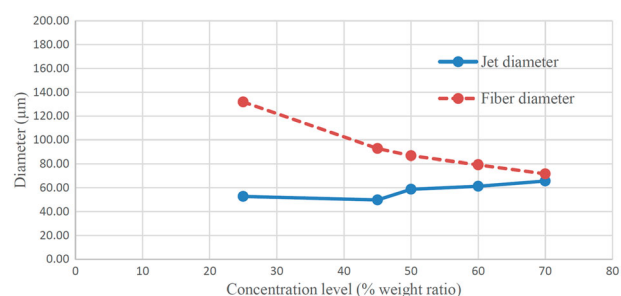


**Figure 13.** Comparison of jet and dry fibre diameters at different concentration levels with compressed air supplied.

at 45% which gave the smallest diameter for gravity flow. More importantly, the gap between the two diameters was closer and closer when the concentration increased which means that the fibre could maintain its shape better. This also reflects by the transformation ratio (TR) that moved from 4.23 at 25% concentration to 1.40 at 70% concentration.

## Two-way ANOVA: Fiber Diameter versus Fabricating Condition, Concentration level

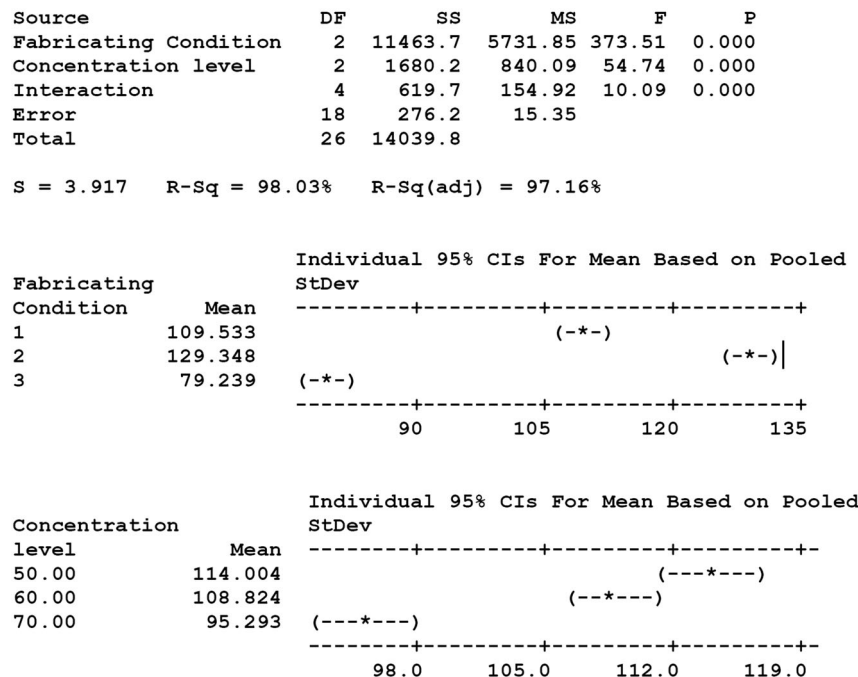


**Figure 14.** Two-way ANOVA test on dry fibre diameter regarding concentration level and fabrication condition.

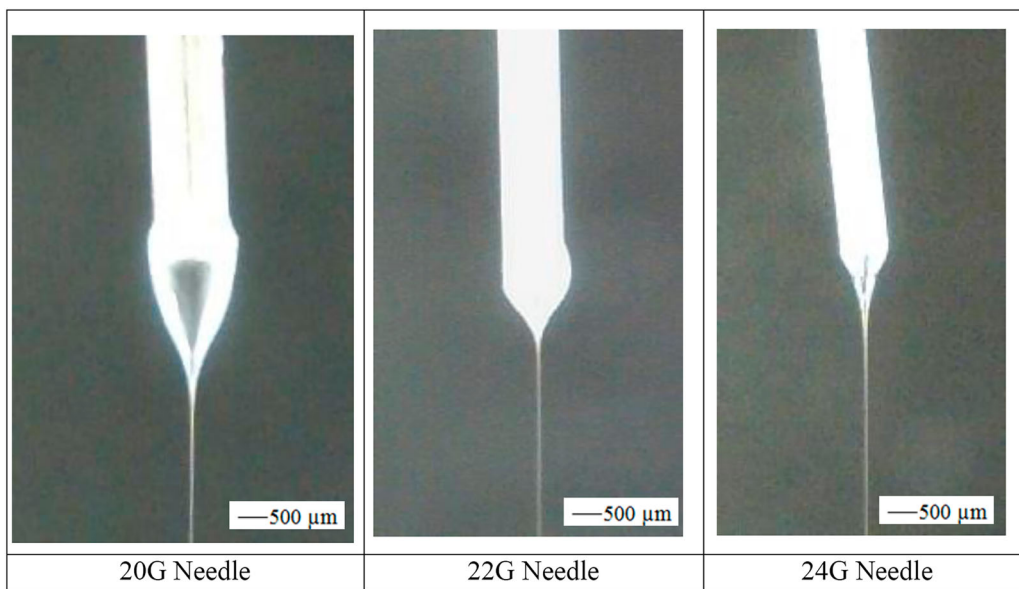


**Figure 15.** Jets obtained at 45% weight of PCL at three different needle sizes.

The gap, however, was still high. Increasing polymer concentration alone could not achieve a cylindrical shape fibre. Therefore, some other parameters need to be taken into account. According to the observation, there was a rise of temperature during the fibre

fabrication from 26°C to 28°C. It could play an important role in solidification time and resulted in jet expansion on the collector before solidifying. Therefore, next set of experiments were focused on environmental condition during the fabrication.

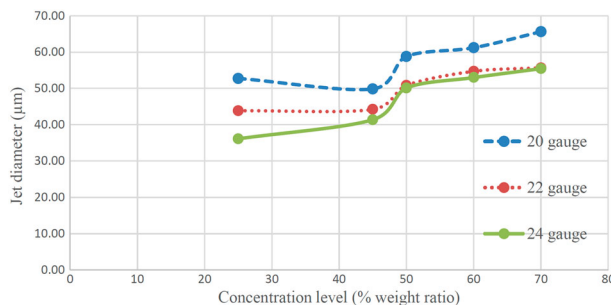


**Figure 16.** Comparison of needle size and concentration level on polymer jet's diameter.

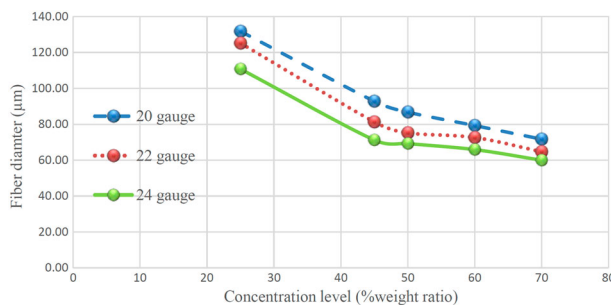


**Figure 17.** Comparison of needle size and concentration level on dry fibre's diameter.

#### 4.4. Environmental condition during the fabrication

Besides normal condition used in all previous experiments, two additional conditions were investigated: introduction of warm air and of compressed air to the process. For this particular experiment, the 20G needle was used, and the SOD was 10 mm. Six similar polymer concentration levels were also used to compare with the normal condition. Also, the supplied voltage was between 3.2 and 3.5 kV for the concentration up to 50% of PCL, and between 3.8 and 4.0 kV for higher concentration. Either warm air or compressed air was introduced into the working area from the bottom.

For the warm air condition, after warm air was blown underneath the platform into the working area, the temperature was increased from 26°C to 33°C, and the humidity was around 40–45%. During the process, the temperature was raised up to 35°C. The experimental results are presented in Figures 8 and 9. The fibre could not be formed from the solution with the 25% concentration level. The jet sprayed the solution instead after travelling some distance from the needle tip. The fibre, however, could be formed at higher concentration levels. Similar experience of early solidification was found for the attempt with the 80% concentration level. The measurement results are shown in Table 5 and Figure 10. It appears that warm dry air thinned the polymer

jet from gravity flow feeding but did not affect the jet from mechanical feeding, and the rising temperature on the collector hindered the solidification of the fibre and allowed the deposited jet to expand. As a result, the fibre diameters were larger relative to those obtained for the same concentration levels under normal condition. Although the TR decreased as the concentration level increased but the value was much higher than the one under normal condition.

For the compressed air condition, the air was also blown from the bottom. The temperature was at 25°C after supplying the air and remained unchanged throughout the process. The humidity was around 70–75%. The experimental results are presented in Figures 11 and 12. The temperature increased the viscosity of the solution. Therefore, the jet became larger and larger with increasing concentration levels. The jet formed with less and less amount of solvent, and underwent rapid solidification. This also means that the dry fibre size was closer to the jet size due to low expansion on the collector. Table 6 shows the measurement results. Therefore, a significant decrease of dry fibre diameter was observed with increasing the concentration level. At the 70% concentration level, the dry fibre of 71.68 μm diameter was formed from the jet of 65.64 μm diameter giving a TR of 1.09. Figure 13 shows that the gap was narrowed down significantly between the jet diameter and dry fibre diameter. This means that the initial cylindrical shape of the jet was much better maintained.

Two-way ANOVAs were conducted to examine the effects of fabrication condition and concentration to the dry fibre diameter. The ANOVA result, as shown in Figure 14, confirms that both factors and their interaction have significant effect on the diameter because the null hypotheses of fabrication condition could be rejected with 95% CI (i.e. the *p*-values were less than .05). According to the experimental results and statistical analysis, supplying compressed air during the process is recommended, and high polymer concentration is required to obtain a small cylindrical fibre.

#### 4.5. Needle size

After knowing the appropriate environmental condition and suitable polymer concentration, this experiment was conducted with an attempt to further reduce the diameter of the fibre. The focus was moved to reducing the initial jet diameter. The amount of material ejected from the needle to some extent is controlled by the needle size. Therefore this experiment investigates the effect of the needle size. Three different needles, 20G, 22G and 24G, were selected. Their inner diameters are 603, 413 and 311 μm, and their outer diameters are

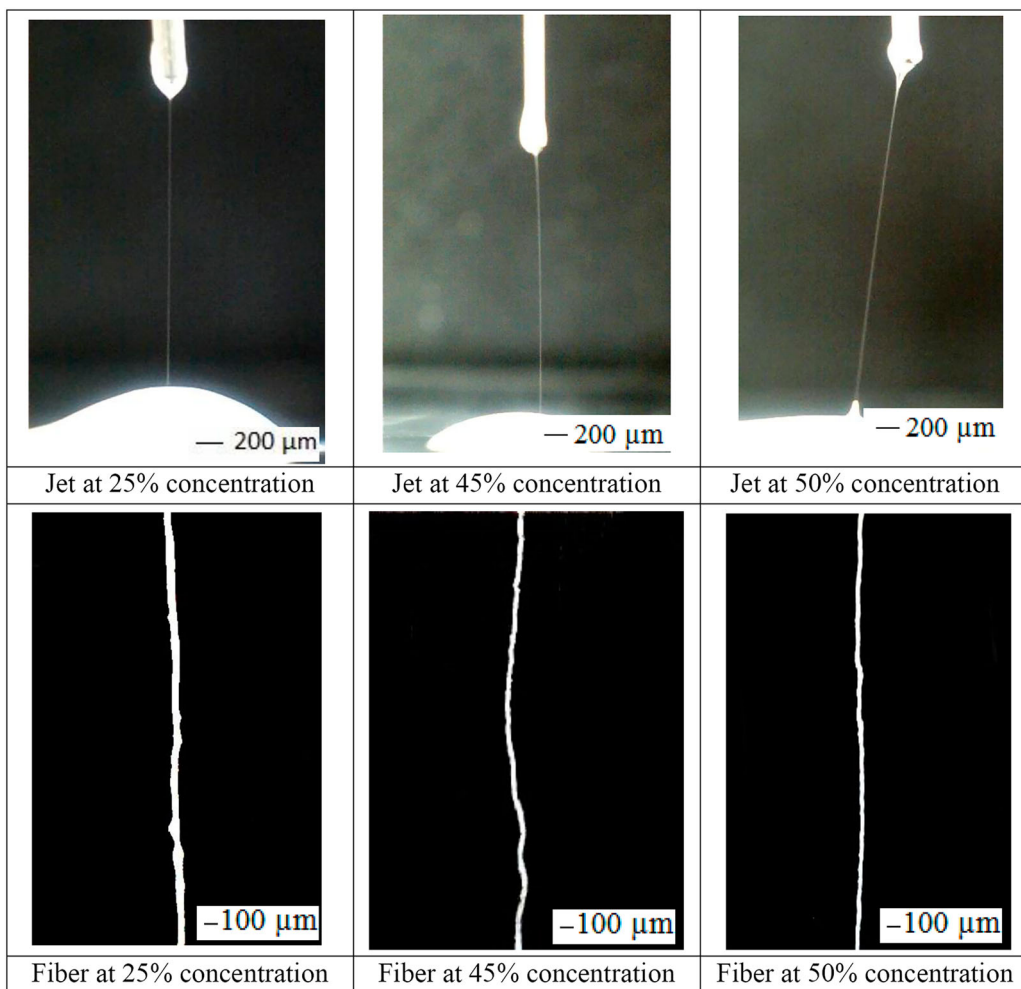


**Figure 18.** Polymer jets and dry fibres created using 24G needle at 25%, 45% and 50% concentration levels with compressed air supplied.

908, 717 and 565  $\mu\text{m}$ , respectively. The SOD was 10 mm and compressed air was supplied during the process. The temperature was at 25°C, and the humidity was around 70–75%. Five polymer concentration levels, 25%, 45%, 50%, 60% and 70% were used. The syringe pump was applied for the concentration of 50% and higher. A feed rate was 1.21  $\mu\text{l/s}$ . The supplied voltage was between 3.2 and 3.5 kV for the PCL concentration of 25%, 45% and 50%, and between 3.8 and 4.0 kV for the PCL concentration of 60% and 70%.

The jet could be created and fibre could be formed for all combinations. Figure 15 illustrates the jet obtained at 45% weight of PCL at the three different needle sizes. The droplet size and shape were quite different. The experimental results are illustrated in Figures 16 and 17. It is clear that the needle size has influence on both jet's and dry fibre's diameter. The smaller the needle size, the smaller the jet and dry fibre will be. Figures 18 and 19 show the jets and dry fibres obtained when 24G needle was used. The smallest jet and dry fibre

with closer diameter to each other was achieved from this needle size. The dry fibre of 59.96  $\mu\text{m}$  was achieved from this needle with the TR of 1.08 at the 70% concentration level as reported in Table 7.

Figure 20 shows a 20-layer scaffold fabricated by using 24G needle to feed a solution of 70% weight ratio of PCL in DMF. The SOD was 10 mm and compressed air was supplied. The humidity and temperature were 70–75% and 25°C, respectively, at the time of scaffold fabrication. The gap size was maintained at 1 mm. Because the jet almost solidified when it reached the collector, no liquid solution was left on the collector. Fibres can be observed and horizontal gaps can be seen clearly between the fibres. Also because the fibres were not completely solidified, they did not have enough strength to maintain their shapes when they sat on the other fibres that were far apart. Therefore, the fibres had a tendency to deflect and attach to adjacent fibres below due to gravity force. Consequently, the third dimension of

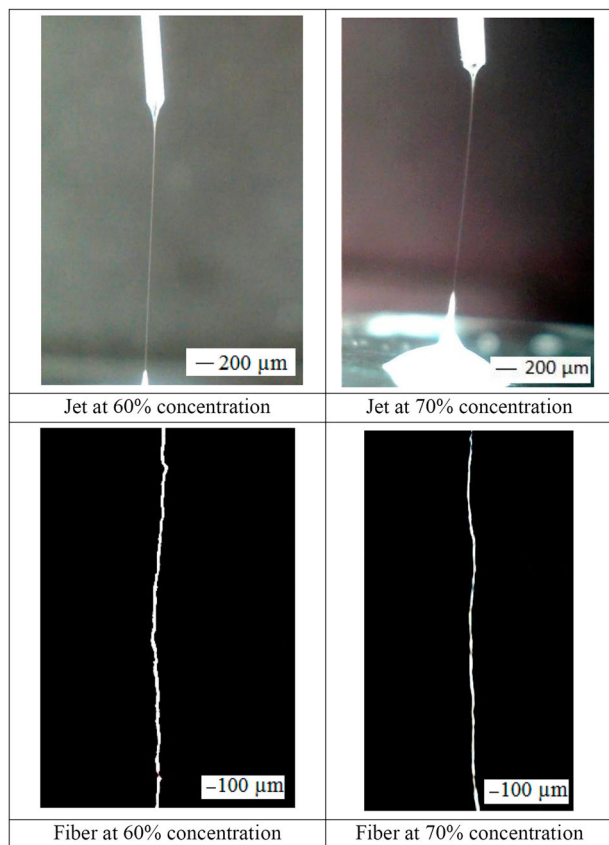


**Figure 19.** Polymer jets and dry fibres created using 24G needle at 60% and 70% concentration levels with compressed air supplied.

the scaffold cannot yet be seen clearly. The precision of a fibre deposition also had an influence. The fibres were not placed accurately on top of the previous ones. This problem to certain extent related to the limitation of the mechanism of a platform.

## 5. Conclusions

Experiments were successfully conducted on the machine prototype of an ESRP technique. The results showed that for NFES polymer concentration, environmental condition and needle size had strong influence on obtaining small cylindrical fibres while voltage and SOD did not. The role of voltage seems to be for initiating a polymer jet. A short SOD does not allow whipping action and limits the evaporation of solvent. Therefore, the polymer concentration should be high to form a fibre quickly prior to arrival at the collector. The temperature that tends to increase during the process should be maintained to help the solidification of the fibre. The smaller the needle is, the smaller the fibre will be. Also there is a proper pairing of concentration and SOD. For instance, 10 mm SOD seems to be suitable for the

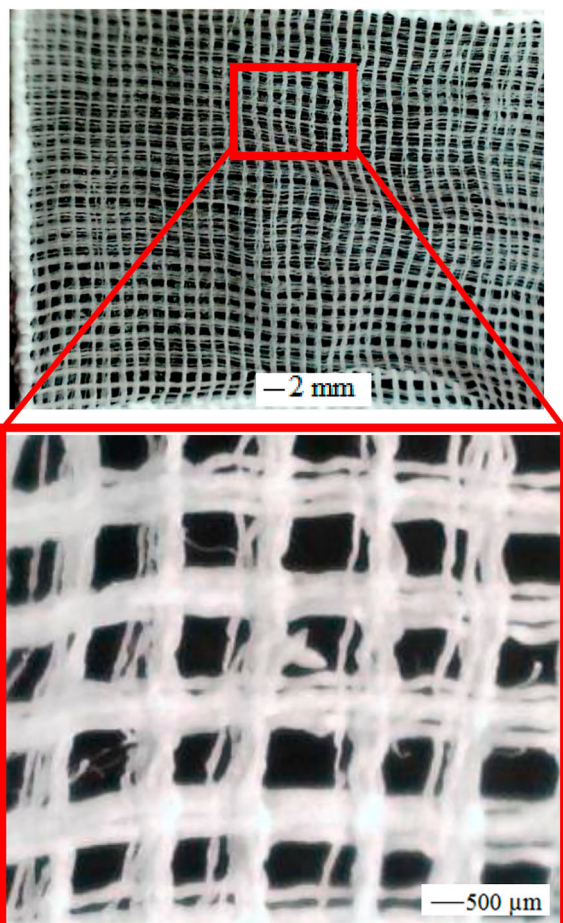


**Figure 20.** Scaffold with 20 layers.

concentration of around 70% weight ratio of PCL in DMF. At this SOD, lower concentrations result in liquid fibre on the collector and higher concentrations result in complete solidification prior to arrival at the collector. Further investigation will be conducted to determine the relationship between polymer concentration and SOD.

## Disclosure statement

No potential conflict of interest was reported by the authors.

## References

- Auyson, K., et al., 2013. Investigation of applying electrospinning in fused deposition modeling for scaffold fabrication. In: P.J. Bartolo, et al., ed. *High value manufacturing: advanced research in virtual and rapid prototyping: Proceedings of the 6th international conference on advanced research in virtual and rapid prototyping*, October, 2013, Leiria, Portugal. Leiden: CRC Press, 149–154.
- Bain, S. and Koomsap, P., 2016. Preliminary study on solvent effect in fiber fabrication in near-field electrospinning. In: C.K. Chua, et al., ed. *Proceedings of the 2nd international conference on progress in additive manufacturing*, May 2016, Singapore. Singapore: Research Publishing, 415–420.

- Bisht, G.S., et al., 2011. Controlled continuous patterning of polymeric nanofibers on three-dimensional substrates using low-voltage near-field electrospinning. *Nano Letters*, 11, 1831–1837.
- Bu, N., et al., 2012. Continuous tunable and oriented nanofiber direct-written by mechano-electrospinning. *Materials and Manufacturing Processes*, 27, 1318–1323.
- Cai, S., et al., 2013. Novel 3D electrospun scaffolds with fibers oriented randomly and evenly in three dimensions to closely mimic the unique architectures of extracellular matrices in soft tissues: fabrication and mechanism study. *Langmuir*, 29 (7), 2311–2318.
- Chang, C., Limkrallassiri, K., and Lin, L., 2008. Continuous near-field electrospinning for large area deposition of orderly nanofiber patterns. *Applied Physics Letters*, 93 (12), 123111 doi:10.1063/1.2975834.
- Chanthakulchan, A., et al., 2015a. Development of an electrospinning-based rapid prototyping for scaffold fabrication. *Rapid Prototyping Journal*, 21 (3), 329–339.
- Chanthakulchan, A., et al., 2015b. Environmental effects in fiber fabrication using electrispinning-based rapid prototyping. *Virtual and Physical Prototyping*, 10 (4), 227–237.
- Chen, R., et al., 2009. A novel approach via combination of electrospinning and FDM for tri-leaflet heart valve scaffold fabrication. *Frontiers of Materials Science in China*, 3 (4), 359–366.
- Doshi, J. and Reneker, D.H., 1995. Electrospinning process and applications of electrospun fibers. *Journal of Electrostatics*, 35, 151–160.
- Gu, S.Y., Ren, J., and Vancso, G.J., 2005. Process optimization and empirical modeling for electrospun polyacrylonitrile (PAN) nanofiber precursor of carbon nanofibers. *European Polymer Journal*, 41, 2559–2568.
- Hasan, A., et al., 2014. Electrospun scaffolds for tissue engineering of vascular grafts. *Acta Biomaterialia*, 10 (1), 11–25.
- Kameoka, J., et al., 2003. A scanning tip electrospinning source for deposition of oriented nanofibers. *Nanotechnology*, 14, 1124–1129.
- Katti, D.S., et al., 2004. Bioresorbable nanofiber-based systems for wound healing and drug delivery: optimization of fabrication parameters. *Journal of Biomedical Materials Research*, 70B, 286–296.
- Koombhongse, S., Liu, W., and Reneker, D.H., 2001. Flat polymer ribbons and other shapes by electrospinning. *Journal of Polymer Science: Part B: Polymer Physics*, 39, 2598–2606.
- Lam, C.X.F., et al., 2002. Scaffold development using 3D printing with a starch-based polymer. *Materials Science and Engineering: C*, 20 (1–2), 49–56.
- Li, J.L., et al., 2014. Fabrication of three-dimensional porous scaffolds with controlled filament orientation and large pore size via an improved E-jetting technique. *Journal of Biomedical Materials Research B: Applied Biomaterials*, 102B (4), 651–658.
- Loh, Q.L. and Choong, C., 2013. Three-dimensional scaffolds for tissue engineering applications: role of porosity and pore size. *Tissue Engineering Part B: Reviews*, 19 (6), 485–502.
- Owida, A., et al., 2011. Artery vessel fabrication using the combined fused deposition modeling and electrospinning techniques. *Rapid Prototyping Journal*, 17 (1), 37–44.
- Padmanabhan, T., et al., 2011. Experimental investigation on the operating variables of a near-field electrospinning process via response surface methodology. *Journal of Manufacturing Processes*, 13, 104–112.
- Park, S.H., et al., 2008. Development of dual scale scaffolds via direct polymer melt deposition and electrospinning for applications in tissue regeneration. *Acta Biomaterialia*, 4 (5), 1198–1207.
- Rogina, A. 2014. Electrospinning process: versatile preparation method for biodegradable and natural polymers and bio-composite systems applied in tissue engineering and drug delivery. *Applied Surface Science*, 296, 221–230.
- Sun, D.H., et al., 2006. Near-field electrospinning. *Nano Letters*, 6, 839–842.
- Tellis, B.C., et al., 2008. Trabecular scaffolds created using micro CT guided fused deposition modeling. *Materials Science and Engineering: C*, 28 (1), 171–178.
- Thavasi, V., Singh, G., and Ramakrishna, S., 2008. Electrospun nanofibers in energy and environmental applications. *Energy and Environmental Science*, 1, 205–221.
- Thompson, C.J., et al., 2007. Effects of parameters on nanofibers diameter determined from electrospinning model. *Polymer*, 38, 6913–6922.
- Too, M.H., et al., 2002. Investigation of 3D non-random porous structures by fused deposition modeling. *International Journal of Advanced Manufacturing Technology*, 19 (3), 217–223.
- Wei, C. and Dong, J., 2013. Direct fabrication of high-resolution three-dimensional polymeric scaffolds using electrohydrodynamic hot jet plotting. *Journal of Micromechanics and Microengineering*, 23, 025017. doi:10.1088/0960-1317/23/2/025017
- Zheng, G., et al., 2016. Electrohydrodynamic direct-writing microfiber patterns under stretching. *Applied Physics A*, 122 (2), 1–9.